TITLE PAGE

Citation Format:

Paiè, P., Calvarese, M., Ceccarelli, F., Sala, F., Bassi, A., Osellame, R., & Bragheri, F. (2022, March). Integrated fast optical switch fabricated by femtosecond laser micromachining. In Frontiers in Ultrafast Optics: Biomedical, Scientific, and Industrial Applications XXII (Vol. 11991, pp. 22-27). SPIE. (February 2022)

Copyright notice:

DOI abstract link:

https://doi.org/10.1117/12.2609037

PROCEEDINGS OF SPIE

SPIEDigitalLibrary.org/conference-proceedings-of-spie

Integrated fast optical switch fabricated by femtosecond laser micromachining

Petra Paiè, Matteo Calvarese, Francesco Ceccarelli, Federico Sala, Andrea Bassi, et al.

Petra Paiè, Matteo Calvarese, Francesco Ceccarelli, Federico Sala, Andrea Bassi, Roberto Osellame, Francesca Bragheri, "Integrated fast optical switch fabricated by femtosecond laser micromachining," Proc. SPIE 11991, Frontiers in Ultrafast Optics: Biomedical, Scientific, and Industrial Applications XXII, 1199105 (4 March 2022); doi: 10.1117/12.2609037

SPIE.

Event: SPIE LASE, 2022, San Francisco, California, United States

Integrated fast optical switch fabricated by femtosecond laser micromachining

Petra Paiè[a], Matteo Calvarese[a,b], Francesco Ceccarelli[a], Federico Sala[b,a], Andrea Bassi[b,a], Roberto Osellame[a,b] and Francesca Bragheri[a,*]
[a] Istituto di Fotonica e Nanotecnologie, IFN-CNR, IT- 20133, Milano, Italy;
[b]Politecnico di Milano, IT- 20133 Milano, Italy

ABSTRACT

Integrated optical switches and modulators allow performing reconfigurability in integrated circuits, resulting as fundamental components in different fields ranging from optical communications to sensing and metrology. Among different methods, the thermo-optic effect has been successfully used to fabricate optical modulators by femtosecond laser micromachining (FLM) in glass substrates, proving high stability, no losses dependance but long switching time. In this work, we present an integrated optical switch realized by FLM with a switching time of less than 1 ms: which is about 1 order of magnitude faster than the other devices present in literature. This result has been achieved by carefully optimizing the geometry and the position of resistors and trenches near the waveguides through simulation and experimental validation. In addition, by means of an optimization of the applied voltage signal, we have demonstrated a further significant temporal improvement, measuring a switching time of less than 100 μs.

Keywords: thermal shifter, integrated optics, femtosecond laser micromachining.

1. INTRODUCTION

Integrated circuit reconfigurability is of paramount importance for a wide range of applications, including optical communications, sensing, metrology and even lab on a chip [1]. Several technologies and materials are currently used for integrated optics applications. Whether the material possesses high nonlinear or electro-optic coefficients, Kerr or Pockels effects can be exploited to achieve light modulation [2]. Otherwise, plasma effects, as in silicon photonics, or thermo-optic effects can be used. The latter technique has been successfully exploited to fabricate optical modulators in glass substrates. This method, which is based on the temperature dependence of the refractive index, guarantees high stability, implementation simplicity, and modulation accuracy, but it is characterized by slow dynamic responses. Among different fabrication techniques femtosecond laser micromachining stands out for its versatility and 3D capabilities, resulting in a valuable alternative to standard lithographic approaches [3]. This technique is based on non-linear absorption processes that occur when focusing a femtosecond laser beam on transparent substrates, such as glasses. This leads to a permanent modification of the substrate in the focal volume, the type of induced modification depends on the irradiation parameters. Among the possible structural changes, a localized refractive index increase with respect to the pristine material can be induced, which enables direct waveguide writing [4]. In addition, FLM allows fabricating both integrated optics and microfluidic channels, which can be used in synergy for the realization of advanced lab-on-a-chip devices in fused silica and borosilicate glasses [5-7]. This technique has been successfully used to fabricate optical modulators in glass substrates [8-11]. These devices are based on the combination of an integrated Mach–Zehnder interferometer (MZI) and a superficial resistor used to asymmetrically heat the arms of the interferometer, and therefore to actively vary the phase difference used for light modulation. In this work, we present an integrated optical switch realized by FLM with a switching time of less than 100 μs, while the circuits in literature are characterized by switching times of the order of tens or hundreds of milliseconds. This result has been achieved by simulating the dynamic response of different geometries with COMSOL Multiphysics, by fabricating and characterizing all the simulated devices and by introducing a pulse-shaping approach in the driving voltage. The rapid prototyping capabilities and the precision of FLM in glass microstructuring have been fundamental for the fabrication of the integrated optical circuits, the trenches and the resistors, allowing a precise optimization in terms of both switching velocity and dissipated power.

Frontiers in Ultrafast Optics: Biomedical, Scientific, and Industrial Applications XXII,
edited by Peter R. Herman, Roberto Osellame, Adela Ben-Yakar, Proc. of SPIE
Vol. 11991, 1199105 · © 2022 SPIE · 0277-786X · doi: 10.1117/12.2609037

2. MATERIALS AND METHODS

2.1 Device Fabrication

The fabrication is a multi-step process, whose protocol is reported hereunder: i) MZI irradiation by FLM, ii) waveguide thermal annealing in oven, iii) superficial gold deposition, and iv) selective gold ablation to define the resistors pattern. The substrate used is a borosilicate glass (Eagle XG, Corning). The femtosecond laser source that we have used is a Yb:KYW cavity-dumped mode-locked laser oscillator, with an emission wavelength of 1030 nm, pulse duration of 300 fs, and a repetition rate of 1 MHz. For waveguide irradiation, we have used a 50x, 0.65 NA microscope objective to focus the laser beam, an average laser power of 230 mW, a scan velocity of 40 mm/s and a multiscan approach based on 12 overlapping irradiations. The waveguides have been irradiated at a distance of 15 μm from the bottom surface of the glass substrate. After the irradiation process we have exposed the substrate to a previously optimized annealing process. The resulting waveguides are characterized by propagation losses of about 0.3 dB/cm and symmetric mode dimensions of about 2.7 x 2.8 μm^2 at a wavelength of 532 nm. We have fabricated different integrated couplers to retrieve the coupling coefficient, we have obtained that fixing the separation between the two arms to 5 μm in the coupling region, an interaction length of 0.75 mm is necessary for a 50:50 splitting ratio. Regarding the ubiquitous metal deposition process, first 2 nm of chromium have been deposited over the substrate to enhance gold to glass adhesion. Subsequently, 80 nm of gold have been deposited using a magnetron sputtering system. A thermal annealing process up to 500 °C, previously optimized, has been introduced to favor the resistors stability over time [12,13]. The ablation for the resistor layout is carried out by using the above-mentioned femtosecond laser, a 10x, 0.25 NA focusing objective, 200 mW of average laser power and 2 mm/s scan velocity. The resistor is 3 mm long and 15 μm large, which corresponds to a resistance value of about 115 Ω. For the fabrication of superficial trenches multiple lines have been irradiated with an average laser power of 800 mW and a scan velocity of 0.2 mm/s. In particular, 5 overlapping scans have been repeated at different depths from the surface, covering the entire height of the trench with an inner separation of 2 μm along the vertical axis (z axis in Fig. 1).

2.2 Device design

To obtain an integrated modulator we have used a MZI, as in Fig. 1, with a heater (i.e. a resistor) fabricated above one of the two arms. Thanks to the thermo-optic effect, it is possible to induce a controlled phase difference in the two arms of the interferometer, therefore it is possible to modify the output power distribution, switching between bar and cross state (P_{bar} and P_{cross} in Fig. 1). Indeed, the transfer matrix of the MZI depends sinusoidally on the phase difference between the two arms and the temperature dependence of the refractive index can be reasonably approximated linear as it follows:

$$P_{bar} = P_{IN}\sin^2\left(\frac{\Delta\phi}{2}\right) \quad (1)$$

$$P_{cross} = P_{IN}\cos^2\left(\frac{\Delta\phi}{2}\right) \quad (2)$$

$$n(T) = n(T_0) + \alpha(T - T_0) \quad (3)$$

Considering that the waveguides are asymmetrically heated, they reach a different temperature, and this translates in the following temperature dependent phase difference:

$$\Delta\phi_{\Delta T} = \frac{2\pi}{\lambda}\alpha L \Delta T \quad (4)$$

where L is the resistor length, and λ the wavelength guided in the MZI. Therefore, by applying a certain voltage over the resistor, it is possible to control the light distribution at the MZI output, switching between the two ports. To optimize the dynamic response, we have focused first in optimizing the layout of the device in its standard configuration (Fig 1.a). This has been done by optimizing the values of Δz and Δx, which are the depth in the substrate at which the waveguides are irradiated and the distance among the two arms, respectively. Subsequently, we have explored advanced configurations, characterized by the presence of a conductive layer above the second waveguide and superficial trenches.

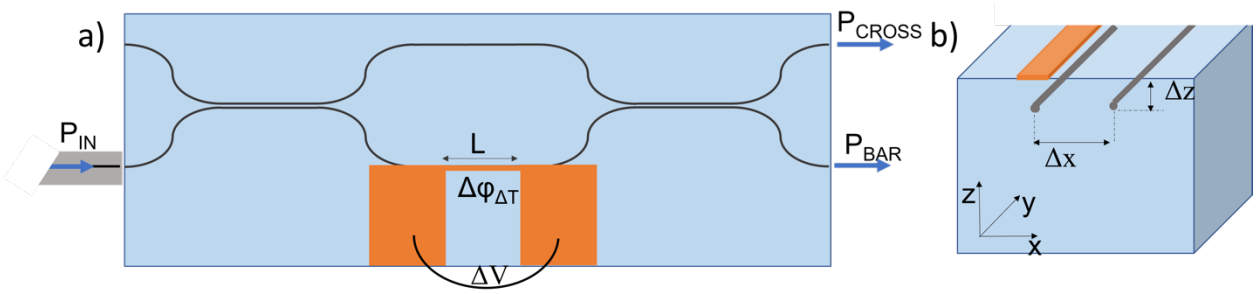

Fig. 1 Top a) and lateral b) view of the schematic of the MZI device in the standard configuration. Δz and Δx correspond to the depth of the waveguides from the surface and the reciprocal distance.

2.3 Device simulations

COMSOL Multiphysics has been used to simulate both the static and dynamic response of the devices to an applied power step. The Heat transfer module allowed to investigate the temperature distribution in the substrate in correspondence of a certain dissipated power. To model the device, three different domains have been introduced. A block of borosilicate glass with dimensions of 5mm x 5mm x 1mm (L x W x H in Fig 2.a), a thin layer of gold of 3mm x 15µm x 1µm (l x w x h in Fig 2.a), set as heat source with an emitting power P and a layer of air 5mm x 5mm x 0.3mm above the others to consider the effect of heat dissipation by conduction in air.

3. RESULTS AND DISCUSSION

3.1 Simulations

Using Comsol simulations we have first investigated how the distance between the waveguides and the superficial resistors as well as the inner distance between the waveguides in the heated area, namely Δz and Δx, affect the device dynamic and the maximum difference in temperature (ΔT) that can be achieved between the two waveguides. Indeed, the objective of this work consists in improving the temporal response of the optical switch, maintaining good values for power dissipation. From this first analysis we have retrieve that minimizing Δz positively affects both power dissipation and temporal response, while we observe an opposite trend regarding the distance between the waveguides. Indeed, at a fixed Δz, it is important to enhance Δx to maximize the difference of temperature reached (ΔT). Conversely, to speed up the dynamics, the two arms should be as close as possible, thus allowing to reach the steady state condition faster. We have chosen to fabricate the integrated MZI at the shallowest possible depth that does not cause surface ablation when writing the waveguides. In our case, this depth corresponds to 15 µm from the surface. At this depth, the reasonable values of Δx which allow a good compromise between dynamics and power dissipation range from 23 to 43 µm, we have therefore selected a distance between the waveguides of 30 µm. Using these parameters, we obtain a device that can switch between bar and cross with a power dissipation of 197 mW and that reaches the 90% of the steady state condition in about 2.4 ms, we will refer to this layout as the *Standard* one. Subsequently, we have explored the possibility of further improving the device performances using *advanced configurations* characterized by the presence of superficial trenches surrounding the resistor as well as a gold conductive nanolayer between the waveguides (slab).

The results of this analysis are illustrated in Fig.2, where it is possible to observe the cross section of two configurations, panels a) and b), and the dynamic comparison Fig.3.c. It is possible to note that these advanced configurations present improved performances with respect to the standard configuration previously described. Indeed, not only the switch is achieved with less power consumption, 132 mW and 118 mW, but also the dyamics is faster as the 90% of the steady state condition is reached in 1.5 and 1 ms for the *Symmetric* and *Asymmetric* device, respectively. In particular, between these two new configurations, the *Asymmetric* device, characterized by two different trenches surrounding the resistor, is the one with better performances.

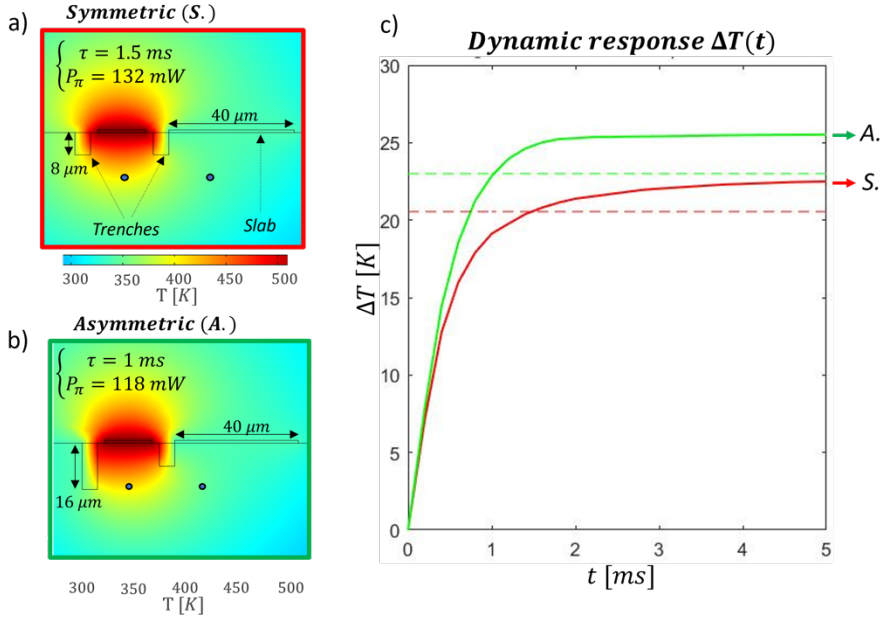

Fig. 2 comparison between the Symmetric and the Asymmetric configurations: temperature distribution in the two cross sections a) and b) and dynamic response c).

3.2 Experimental validation

We have subsequently validated our simulation fabricating the *Standard*, the *Symmetric* and the *Asymmetric* configuration and we characterized the corresponding performances by measuring the power required to perform a switch as well as the temporal response. Regarding the power dissipation we measured 230 mW for the *Standard* configuration and 155 mW for both the *Symmetric* and the *Asymmetric* one. These values are slightly higher with respect to the simulated ones; a possible explanation is that this discrepancy could be related to the ubiquitous gold deposition that affects the heat dissipation in real devices. The switching time comparison is shown in Fig. 4, where the three dynamics are reported, and the expected performances are confirmed. As shown, the *Asymmetric* configuration is the fastest one with a switching time of about 830 μs, while the *Symmetric* and the *Standard* ones present a measured switching time of about 1ms and 1.18 ms, respectively. It is worth highlighting that the measured switching times are, as expected, different from τ that

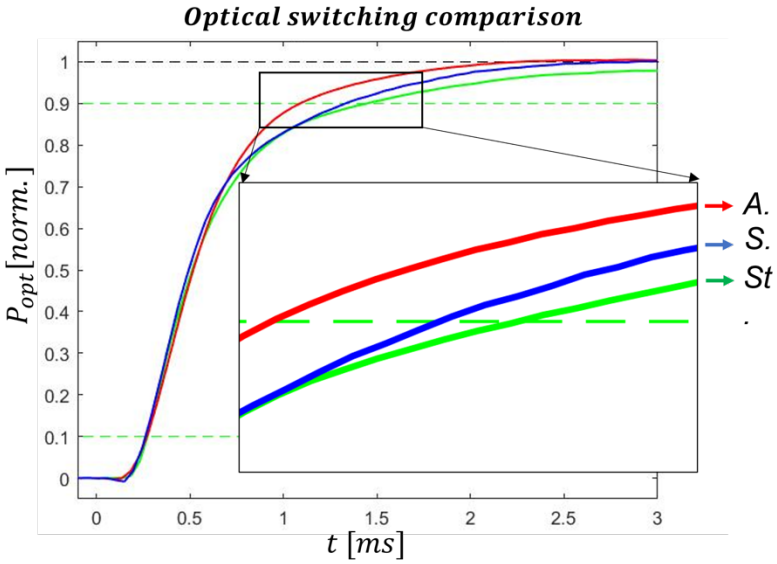

Fig. 3. Experimental comparison between the Standard, Symmetric and Asymmetric switching dynamics.

represent the 90% of the time required to reach the steady state difference of teperature, due to the non-linear response of the MZI over ΔT (see Eq.1,2).

3.3 Voltage function optimization

To further speed up the system we have investigated a pulse shaping approach, thus we have decided to optimize the applied voltage power function to obtain a step-like response of the system. Indeed, instead of applying a step-like voltage, or power, the new function consists in a first peak step, whose duration is optimized to allow the system to reach the required difference of temperature to perform the optical switch, followed by a second step at the regime voltage power, which permits to maintain the previously reached temperature difference. Using this approach and applying it to the *Asymmetric* configuration, we have measured a switching-on time of about 78 μs.

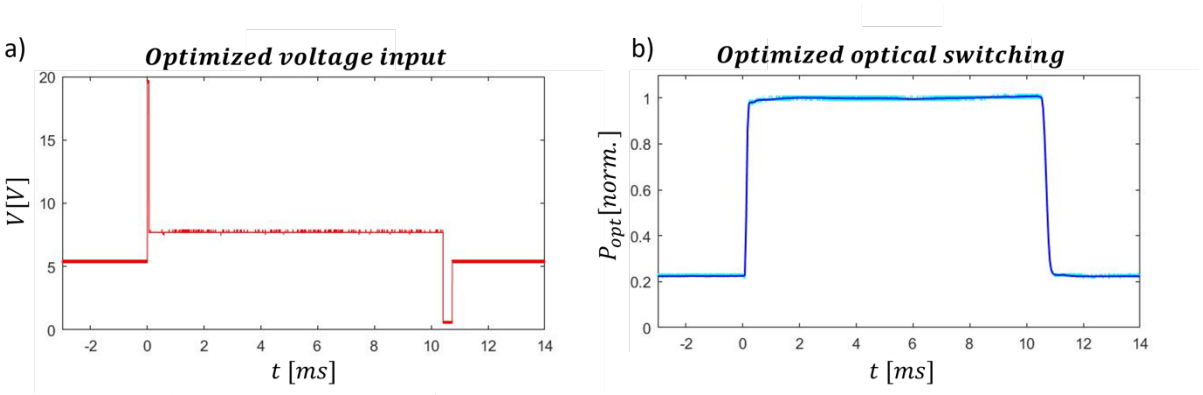

Fig. 4. Optimized voltage input a) and corresponding measured switching dynamics b).

4. CONCLUSIONS

In this work we have been able to improve the switching time of integrated optical switch fabricated by FLM of about two orders of magnitude with respect to the results present in the literature, without sacrificing the power consumption.
Comsol simulations, advanced micro-structuring and voltage function optimization have played a fundamental role in achieving this result.

* francesca.bragheri@ifn.cnr.it; phone +390223996199; fax +390223996126; www.ifn.cnr.it

ACKNOWLEDGMENTS

The fabrication was partially performed at PoliFAB, the micro- and nanofabrication facility of the Politecnico di Milano (www.polifab.polimi.it). The authors would like to thank the PoliFAB staff for the valuable technical support.
We acknowledge financial support by the European Union through the H2020 FET Open project PROCHIP (Grant ID: 801336). R.O. also acknowledges financial support from the European Union through the ERC Advanced project CAPABLE (Grant ID: 742745).

REFERENCES

[1] Bogaerts, W., Pérez, D., Capmany, J., Miller, D.A., Poon, J., Englund, D., Morichetti, F. and Melloni, A. "Programmable photonic circuits," Nature 586(7828), 207-216 (2020).
[2] Wang, C., Zhang, M., Chen, X., Bertrand, M. and Shams-Ansari, A. "Integrated lithium niobate electro-optic modulators operating at CMOS-compatible voltages," Nature 562(7725), 101-104 (2018).

[3] Gattass, R. and Mazur, E. “Femtosecond laser micromachining in transparent materials,” Nat. Photonics 2(4), 219-225 (2008).
[4] Corrielli, G., Crespi, A., Della Valle, G., Longhi, S. and Osellame, R. “Fractional Bloch oscillations in photonic lattices,” Nat. Commun. 4(1), 1-6 (2013).
[5] Sala, F., Castriotta, M., Paiè, P., Farina, A., D’Annunzio, S., Zippo, A., Osellame, R., Bragheri, F. and Bassi, A., “High-throughput 3D imaging of single cells with light-sheet fluorescence microscopy on chip,” Biomedical optics express, 11(8), pp.4397-4407 (2020).
[6] Memeo, R., Paiè, P., Sala, F., Castriotta, M., Guercio, C., Vaccari, T., Osellame, R., Bassi, A. and Bragheri, F., “Automatic imaging of Drosophila embryos with light sheet fluorescence microscopy on chip,” Journal of Biophotonics, 14(3), p.e202000396 (2021).
[7] Crespi, A., Osellame, R. and Bragheri, F., “Femtosecond-laser-written optofluidics in alumino-borosilicate glass”, Optical Materials: X, 4, p.100042 (2019).
[8] Chaboyer, Z., Meany, T., Helt, L.G., Withford, M.J. and Steel, M.J. “Tunable quantum interference in a 3D integrated circuit,” Sci. Rep. 5(1), 1-5 (2015).
[9] Flamini, F., Magrini, L., Rab, A.S., Spagnolo, N., D'ambrosio, V., Mataloni, P., Sciarrino, F., Zandrini, T., Crespi, A., Ramponi, R. and Osellame, R. “Thermally reconfigurable quantum photonic circuits at telecom wavelength by femtosecond laser micromachining,” Light Sci. Appl. 4(11), e354-e354 (2015).
[10] Chaboyer, Z., Stokes, A., Downes, J., Steel, M.J. and Withford, M.J. “Design and fabrication of reconfigurable laser-written waveguide circuits,” Opt. Express 25(26), (33056-33065 (2017).
[11] Ceccarelli, F., Atzeni, S., Pentangelo, C., Pellegatta, F., Crespi, A. and Osellame, R. “Low power reconfigurability and reduced crosstalk in integrated photonic circuits fabricated by femtosecond laser micromachining”. Laser Photonics Rev. 14(10), 2000024 (2020).
[12] Arriola, A., Gross, S., Jovanovic, N., Charles, N., Tuthill, P.G., Olaizola, S.M., Fuerbach, A. and Withford, M.J. “Low bend loss waveguides enable compact, efficient 3D photonic chips”, Opt. Express, 21(3), 2978-2986 (2013).
[13] Corrielli, G., Atzeni, S., Piacentini, S., Pitsios, I., Crespi, A. and Osellame, R. “Symmetric polarization-insensitive directional couplers fabricated by femtosecond laser writing”, Opt. Express, 26(12), 15101-15109 (2018).